

Retraction

Retracted: Research on Output Waveform of Generator with Rectifier Load considering Commutation Overlap Angle

Mathematical Problems in Engineering

Received 25 July 2023; Accepted 25 July 2023; Published 26 July 2023

Copyright © 2023 Mathematical Problems in Engineering. This is an open access article distributed under the Creative Commons Attribution License, which permits unrestricted use, distribution, and reproduction in any medium, provided the original work is properly cited.

This article has been retracted by Hindawi following an investigation undertaken by the publisher [1]. This investigation has uncovered evidence of one or more of the following indicators of systematic manipulation of the publication process:

- (1) Discrepancies in scope
- (2) Discrepancies in the description of the research reported
- (3) Discrepancies between the availability of data and the research described
- (4) Inappropriate citations
- (5) Incoherent, meaningless and/or irrelevant content included in the article
- (6) Peer-review manipulation

The presence of these indicators undermines our confidence in the integrity of the article's content and we cannot, therefore, vouch for its reliability. Please note that this notice is intended solely to alert readers that the content of this article is unreliable. We have not investigated whether authors were aware of or involved in the systematic manipulation of the publication process.

Wiley and Hindawi regrets that the usual quality checks did not identify these issues before publication and have since put additional measures in place to safeguard research integrity.

We wish to credit our own Research Integrity and Research Publishing teams and anonymous and named external researchers and research integrity experts for contributing to this investigation.

The corresponding author, as the representative of all authors, has been given the opportunity to register their agreement or disagreement to this retraction. We have kept a record of any response received.

References

- [1] B. Zhang, G. He, and G. Feng, "Research on Output Waveform of Generator with Rectifier Load considering Commutation Overlap Angle," *Mathematical Problems in Engineering*, vol. 2021, Article ID 9920703, 12 pages, 2021.

Research Article

Research on Output Waveform of Generator with Rectifier Load considering Commutation Overlap Angle

Bingyi Zhang, Gongfei He , and Guihong Feng

School of Electrical Engineering, Shenyang University of Technology, Shenyang 110870, China

Correspondence should be addressed to Gongfei He; hegf2646@163.com

Received 4 March 2021; Revised 31 March 2021; Accepted 15 April 2021; Published 26 April 2021

Academic Editor: Sang-Bing Tsai

Copyright © 2021 Bingyi Zhang et al. This is an open access article distributed under the Creative Commons Attribution License, which permits unrestricted use, distribution, and reproduction in any medium, provided the original work is properly cited.

The purpose of this paper is to study the influence of the uncontrolled rectifier circuit on the generator's output waveform when considering the commutation overlap angle. Taking the nonsalient permanent magnet (PM) generator directly connected with the uncontrolled rectifier circuit as an example, the equivalent circuit of the generator with rectifier load is established, and the commutation process of the rectifier circuit is analyzed when the effect of the commutation overlap angle is considered. The output waveforms of generator's output side are obtained by analytical method, circuit simulation method, field-circuit coupled simulation method, and experimental method. The validity of the analysis methods is demonstrated by comparison. According to the results of analytical analysis, we know the characteristics of the output waveform under the influence of the commutation overlap angle. The existence of the commutation overlap angle will cause the voltage waveform to concave or convex, prolong the conduction time of the winding, and result in phase difference between the voltage waveform and current waveform. The influence of synchronous inductance and extra inductance on the output waveforms and harmonic distortion rate is analyzed. The research of this paper provides a theoretical basis for improving the output waveform of the generator with rectifier load.

1. Introduction

Distributed power supply system as the main power supply or standby power supply is widely used in numerous fields such as marine electric propulsion, wind power generation, aviation, emergency, mine, and petrochemical. When the capacity demand for the distributed power supply is large, the power supply method in parallel operation of electric excitation synchronous generator sets is often adopted. This power supply method needs to adopt constant frequency and constant voltage double-closed loops' control and also needs to balance the active power and reactive power of each set with the load sharing device, and the control system is complex. When using the DC bus power supply system, load sharing of each set can be achieved by simply adjusting the amplitude of generator's output voltage, and there is no need to maintain the frequency of generator's output voltage constant, and the adjustment of the amplitude can be achieved by adjusting the prime mover speed [1]. This provides a convenient condition for the application of the

PM generator with high efficiency, simple structure, large torque density, and many other advantages and also promotes the development of the distributed DC power supply system. There is a rectifier in the distributed DC power supply system, and the existence of the rectifier will cause distortion of the AC side output waveforms of the power supply system and will have a serious impact on generator's performance [2, 3].

The AC side harmonic pollution problem caused by the nonlinear loads such as the rectifier circuit has been paid high attention to. Aimed at different generator types and rectification methods, the researchers use different methods to analyze the output characteristics of the distributed DC power supply system. The pulse width modulation rectifier is the best choice because of the high-quality AC side output waveforms and high power factor, but the cost is high and control is complex [4, 5]. At present, the widely used uncontrolled rectifier will bring harmonic pollution to the power grid side, and the power factor is low, and the existence of a large number of harmonics will lead to an

increase in power line and equipment loss, reduce the efficiency of power generation, transmission, and electrical equipment, and cause equipment vibration and noise worse [6–8], so how to improve the waveforms' quality of the power grid side in the uncontrolled rectifier circuit has been a research hotspot. In the work by Zhang and Wu [9], the working characteristics of the electric excitation synchronous generator with uncontrolled rectifier load are analyzed and the AC side voltage and current waveforms are obtained by numerical simulation. In [10–13], the equivalent circuit model of the power generator system with uncontrolled rectifier load is established, and the mutual influence of voltage and current harmonics is analyzed. In the study by Meyer et al. [14], current waveform characteristics of the power grid side are analyzed by Simulink simulation when the electric vehicle charging pile adopts the uncontrolled rectifier method, and the current waveform quality is improved by using the harmonic compensation device. In the study by Zhang et al. [15], the output characteristics of the electric excitation doubly salient generator are analyzed by the field-circuit coupled simulation method, and the accuracy is verified by experiments.

In summary, the main research methods of AC side output characteristics of the distributed DC power supply system are mainly analyzed method, circuit simulation method, field-circuit coupled simulation method, and experimental method. This paper takes the nonsalient PM generator with the uncontrolled rectifier circuit as an example, and the output voltage and current waveforms of the generator are obtained by using the above methods. The influence mechanism of generator's output waveforms, which is influenced by the rectifier circuit, is analyzed with the solving process of the analytic method, which provides the necessary conditions for studying how to improve the output waveforms of the distributed DC power supply. The comparison of the voltage and current waveforms obtained by each method shows the relative consistency of each method, and the advantages and limitations of each approach are illustrated.

2. Equivalent Circuit of the Permanent Magnet Generator

Whether the generator is connected to rectifier load through the transformer or not, because of the inductance series connection in the circuit, the commutation process cannot be completed instantaneously at the natural commutation point, and the delay phenomenon occurs, and the delay time is expressed by an electric angle γ , which is called the commutation overlap angle. During the commutation period, the total voltage caused by the two-phase short circuit is clamped, which increases the output voltage harmonic content and increases the noncharacteristic harmonics of the output current, resulting in the existence of the phase difference between the output voltage waveform and output current waveform. Therefore, it is necessary to analyze the influence of generator parameters on the commutation overlap angle. When connected to the rectified load through the transformer, only the transformer leakage inductance is

connected in series with the load, whose value can be regarded as a constant. When the generator is directly connected with the rectified load, due to the existence of self-inductance, leakage inductance, and mutual inductance of the windings, the equivalent calculation of the inductance series in the circuit is complicated. Because of the air gap of the salient pole PM generator is not uniform, the self-inductance and mutual inductance of the windings also change with rotor position, so it is difficult to obtain the equivalent circuit of the salient pole PM generator [16].

In order to make the qualitative analysis of the effect of commutation overlap angle on the generator output voltage waveform and current waveform more accurately, it is necessary to determine the equivalent circuit and resistance and inductance parameters of the generator. In the case of the nonsalient pole PM generator, the following assumptions are made before the mathematical model is established: the no-load air gap magnetic field of the generator is sinusoidal, and the influence of the armature reaction magnetic field on the excitation magnetic field is neglected, that is, the no-load EMF of the generator is sinusoidal, and the amplitude is constant, and the permeability of the permanent magnet is a constant, and similar to the permeability of air, the magnetic resistance of the stator and rotor core lamination is neglected [17]. The voltage equations of PM generator three-phase windings can be expressed as

$$\begin{cases} u_a = \frac{d\psi_{fa}}{dt} - \frac{d\psi_a}{dt} - R_s i_a, \\ u_b = \frac{d\psi_{fb}}{dt} - \frac{d\psi_b}{dt} - R_s i_b, \\ u_c = \frac{d\psi_{fc}}{dt} - \frac{d\psi_c}{dt} - R_s i_c. \end{cases} \quad (1)$$

In the formula, R_s is the stator phase resistance, ψ_{fa} , ψ_{fb} , and ψ_{fc} are excitation flux linkages of A-phase, B-phase, and C-phase windings, respectively, and ψ_a , ψ_b , and ψ_c are the total armature reaction flux linkages of A-phase, B-phase and C-phase windings, respectively, and there is

$$\begin{pmatrix} \psi_a \\ \psi_b \\ \psi_c \end{pmatrix} = \begin{pmatrix} L_a & L_{ab} & L_{ac} \\ L_{ba} & L_b & L_{bc} \\ L_{ca} & L_{cb} & L_c \end{pmatrix} \begin{pmatrix} i_a \\ i_b \\ i_c \end{pmatrix}. \quad (2)$$

In the formula, L_a , L_b , and L_c are the self-inductances of A-phase, B-phase, and C-phase windings, respectively, L_{ab} , L_{ac} , L_{ba} , L_{bc} , L_{ca} , and L_{cb} are the mutual inductances between the A-phase, B-phase, and C-phase windings, and i_a , i_b , and i_c are the currents of the A-phase, B-phase, and C-phase windings; based on the assumptions above, there is

$$\begin{cases} L_a = L_b = L_c = L_{s\sigma} + L_{m1}, \\ \frac{L_{ab} = L_{ba} = L_{ac} = L_{ca} = L_{bc} = L_{cb} = -L_{m1}}{2}, \\ i_a + i_b + i_c = 0. \end{cases} \quad (3)$$

In the formula, $L_{s\sigma}$ and L_{m1} are the leakage inductance and excitation inductance of the phase winding; taking A phase as an example, there is

$$\Psi_a = L_a i_a - \frac{1}{2} L_{m1} (i_b + i_c) = L_{s\sigma} i_a + \frac{3}{2} L_{m1} i_a = L_t i_a. \quad (4)$$

In the formula, ($L_t = L_{s\sigma} + 3L_{m1}/2$) is called synchronous inductance, and the voltage vector equation of the stator winding can be obtained by summarizing the derivation formulas above:

$$\dot{U}_a = \dot{E}_a - L_t \frac{di_a}{dt} - R_s i_a. \quad (5)$$

The equivalent circuit of the nonsalient pole PM generator can be obtained according to formula (5). When the current in the winding has a sudden change, the presence of the synchronous inductance will hinder this change, resulting in the existence of the commutation overlap angle, so the magnitude of the commutation overlap angle is related to the self-inductance, leakage inductance, and mutual inductance of the armature windings. Because there is no excitation winding and damping winding on the rotor of the PM generator, the transient inductance of the PM generator is equal to that of the steady state when neglecting the eddy current effect [18].

3. Analysis of the Commutation Process in the Uncontrolled Rectifier Circuit

In the study of the influence of the uncontrolled rectifier circuit on generator's output voltage and current waveforms, many literatures analyze the working process of the uncontrolled rectifier circuit on the basis of different assumptions. In the work by Dai et al. [19], the commutation process of the doubled nonsalient pole electric excitation generator is analyzed, and the analytical formulas of commutation time, the value of commutation overlap angle, and commutation voltage drop are deduced. It is assumed that the DC side current is straight like other literatures. When the DC current is straight as the prerequisite, the output current of the AC side is also a constant during the non-commutation period. In order to simplify the equivalent circuit and facilitate the analytical analysis, taking resistive load as example, the equivalent circuit of the nonsalient PM generator with the uncontrolled rectifier circuit is shown in Figure 1.

In the normal operation of the rectifier circuit, the two diodes in the same phase cannot turn on at the same time, and if there is the state that the commutation overlap angle $\gamma > 60^\circ$, there must be the state that the commutation overlap angle $\gamma < 60^\circ$, and the generator is in an asymmetrical and nonnormal working condition. Therefore, the study in this paper will limit the value of the commutation overlap angle in the range of $0 < \gamma < 60^\circ$. The commutation overlap angle will cause the common anode group or the common cathode group two diodes to conduct simultaneously, and the working state of the three-phase rectifier bridge will be changed from 6 to 12, and the duration of each state is

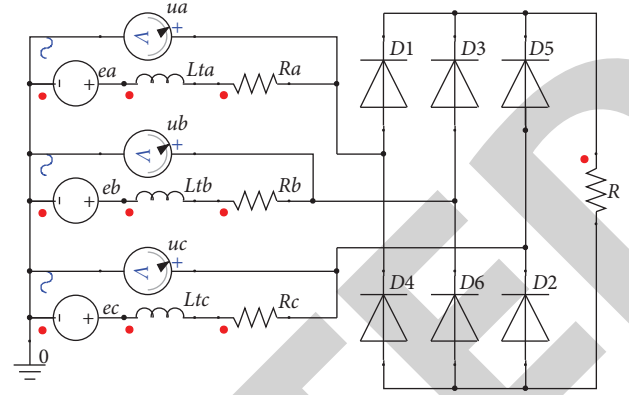


FIGURE 1: Equivalent circuit of the rectifier generator set.

related to the value of the commutation overlap angle. The no-load back EMF waveforms of three phase windings within a single cycle is shown in Figure 2, assume the RMS values as U_2 . According to the symmetry of the circuit structure, it is only necessary to study the output voltage and current waveform in the positive half period of the A-phase winding. It is assumed that the starting point of the commutation overlap angle is the natural commutation point, and the influence of the stator phase resistance is neglected. In the case of $\gamma \leq (\pi/6)$, the output voltage of the A-phase winding rises from zero at the origin.

During the period of $0 \sim (\pi/6)$ according to the diode conduction conditions, only diodes D5 and D6 are conducting, and the equivalent circuit shown in Figure 1 can be simplified to the modal 1 shown in Figure 3, and the transient voltage and current equations of the circuit are

$$\begin{cases} u_a = e_a, \\ i_a = 0. \end{cases} \quad (6)$$

During $(\pi/6) \sim (\pi/6) + \gamma$ period, according to the diode conduction conditions, only diodes D1, D5 and D6 are conducting, and the equivalent circuit shown in Figure 1 can be simplified to the modal 2 shown in Figure 3; in contrast to the sudden increase of current i_a and the sudden reduce of current i_c , it can be temporarily considered that $i_b = i_r$, with little change, that is, $(di_b/dt) = 0$, and the transient voltage and current equations of the circuit are

$$\begin{cases} u_a = e_a - L_t \frac{di_a}{dt}, \\ u_b = e_b - L_t \frac{di_b}{dt} \Rightarrow \begin{cases} u_a = \frac{e_a + e_c}{2}, \\ L_t \frac{di_a}{dt} = \frac{e_a - e_c}{2}, \end{cases} \\ u_c = e_c - L_t \frac{di_c}{dt}. \end{cases} \quad (7)$$

During $(\pi/6) + \gamma \sim (\pi/2)$ period, according to the diode conduction conditions, only diodes D1 and D6 are

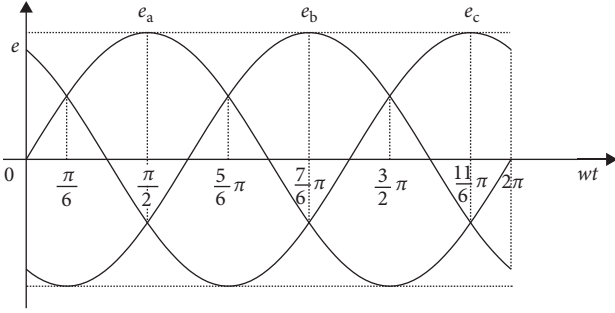


FIGURE 2: No-load back EMF waveform.

conducting, and the equivalent circuit shown in Figure 1 can be simplified to the modal 3 shown in Figure 3, C-phase in cut-off state, there is $i_b = -i_a$, and the transient voltage and current equations of the circuit are

$$\begin{cases} u_r = u_a - u_b = e_a - e_b - 2L_t \frac{di_a}{dt} = i_a R, \\ u_a = e_a - L_t \frac{di_a}{dt}. \end{cases} \quad (8)$$

During $(\pi/2) \sim (\pi/2) + \gamma$ period, according to the diode conduction conditions, only diodes D1, D2 and D6 are conducting, and the equivalent circuit shown in Figure 1 can be simplified to the modal 4 shown in Figure 3, B-phase and C-phase in short circuit state, it can be temporarily considered that $i_a = i_r$ with little change, that is, $(di_a/dt) = 0$. The transient voltage and current equations of the circuit are

$$\begin{cases} u_r = u_a - u_b = u_a - u_c = e_a - \frac{e_b + e_c}{2} = i_a R, \\ u_a = e_a - L_t \frac{di_a}{dt}. \end{cases} \quad (9)$$

During $(\pi/2) + \gamma \sim (5\pi/6)$ period, according to the diode conduction conditions, only diodes D1 and D2 are conducting, and the equivalent circuit shown in Figure 1 can be simplified to a modal similar to the modal 3 shown in Figure 3. The transient voltage and current equations of the circuit are

$$\begin{cases} u_r = u_a - u_c = e_a - e_c - 2L_t \frac{di_a}{dt} = i_a R, \\ u_a = e_a - L_t \frac{di_a}{dt}. \end{cases} \quad (10)$$

During $(5\pi/6) \sim (5\pi/6) + \gamma$ period, according to the diode conduction conditions, only diodes D1, D2 and D3 are conducting, and the equivalent circuit shown in Figure 1 can be simplified to a modal similar to the modal 2 shown in Figure 3. The transient voltage and current equations of the circuit are

$$\begin{cases} u_a = \frac{e_a + e_b}{2}, \\ L_a \frac{di_a}{dt} = \frac{e_a - e_b}{2}. \end{cases} \quad (11)$$

During $(5\pi/6) + \gamma \sim \pi$ period, according to the diode conduction conditions, only diodes D2 and D3 are conducting, and the equivalent circuit shown in Figure 1 can be simplified to a modal similar to the modal 1 shown in Figure 3, and with the same transient voltage and current equations.

The above analysis results show that, under the influence of the commutation overlap angle, the positive half period of the generator output voltage and current waveforms are divided into 7 segments when $\gamma \leq (\pi/6)$. When $(\pi/6) < \gamma < (\pi/3)$, according to the periodicity and continuity of the circuit, the starting point of the $(5\pi/6) + \gamma \sim \pi$ period will be in the next time period, and the starting point of modal 1 working state is $\gamma - (\pi/6)$, and the remaining intervals are piecewise unchanged. The remaining periods remain the same, and the transient voltage and current equations of each period remain the same.

4. Influence of Uncontrolled Rectification on Generator's Output Waveform

4.1. Analytic Analysis of Generator's Output Waveform.

In the commutation process analysis of the uncontrolled rectifier circuit, the instantaneous value expressions of generator output voltage and current of the A-phase winding within the positive half cycle are given. By using these expressions, the output voltage and current waveform of the generator can be drawn so that the influence of the rectifier circuit on the output waveform of the AC side can be understood more intuitively. In order to draw the waveform effectively, it is necessary to determine the value of the commutation overlap angle and the boundary conditions of each segment.

Through the voltage and current equations of the $(\pi/6) \sim (\pi/6) + \gamma$ period, the current expression of the A-phase winding can be obtained:

$$i_a = \frac{\sqrt{6}U_2}{2\omega L_t} \left[1 - \cos\left(\omega t - \frac{\pi}{6}\right) \right]. \quad (12)$$

By modal 1, when $\omega t = (\pi/6)$, the B phase is in the normal conducting state, and $i_{b(\pi/6)} = ((e_c - e_b)/R)$, and during the period of A-phase and C-phase simultaneous conduction, B-phase current varies little, and it can be assumed that $i_{r1} = i_{a((\pi/6)+\gamma)} = i_{b((\pi/6)+\gamma)} = i_{b(\pi/6)}$. According to the boundary condition and the abovementioned formulas, the expressions of the commutation overlap angle can be obtained:

$$\cos \gamma_1 = 1 - \frac{2\omega L_t i_{r1}}{\sqrt{6}U_2}. \quad (13)$$

Using the above approximate γ_1 , i_r can be calculated more accurate that

$$i_r = i_{a((\pi/6)+\gamma)} = \frac{(u_a - u_b)}{R} = 2 \frac{(e_a + e_c)}{R} - \frac{e_b}{R}. \quad (14)$$

An accurate commutation overlap angle can be obtained by substituting i_r into formula (13), and the result can be made more accurate by repeated iterations.

During $(\pi/6) + \gamma \sim (\pi/2)$ period, according to the current equation, the expression of the current can be obtained:

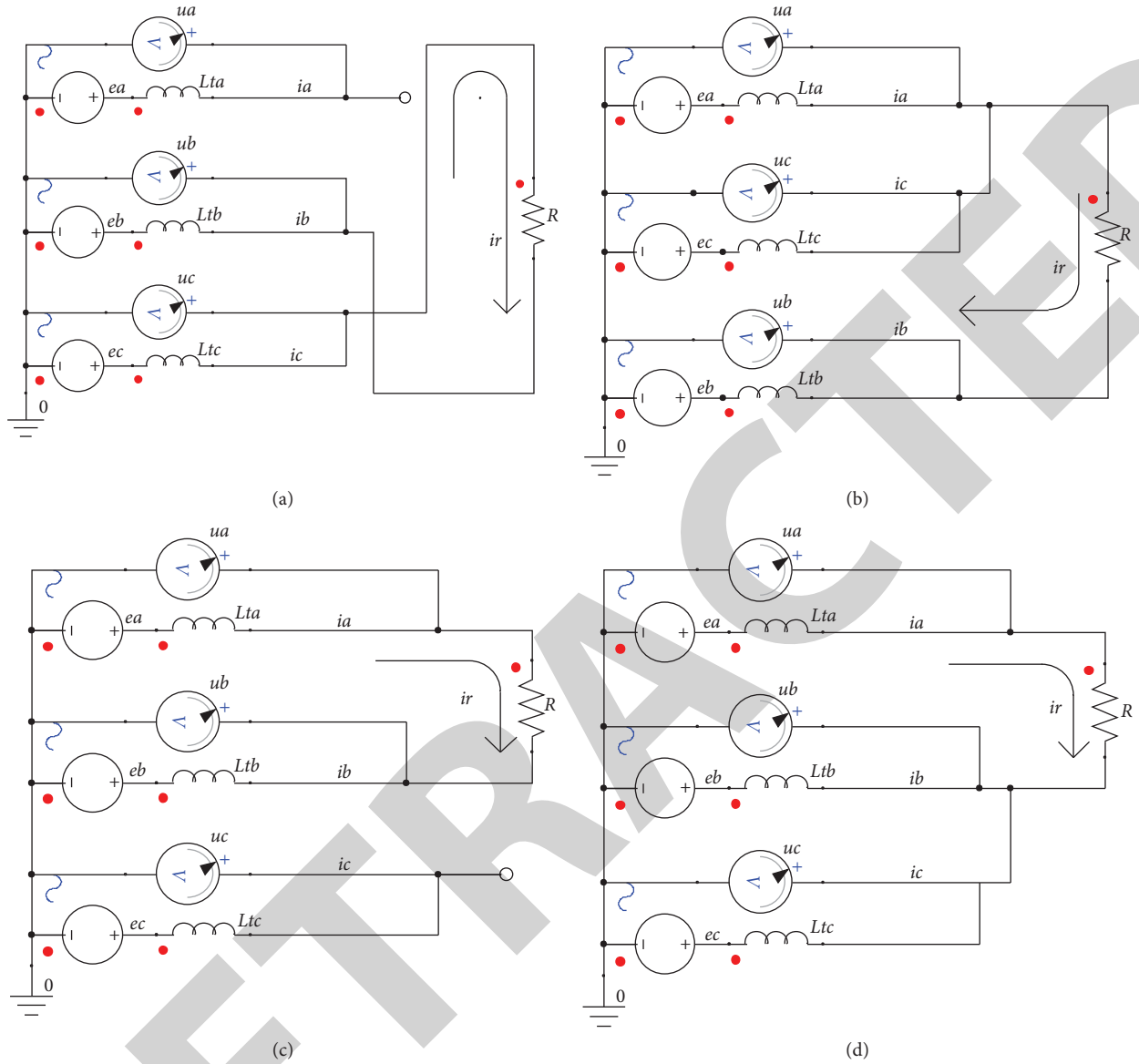


FIGURE 3: (a) Equivalent circuit modal 1. (b) Equivalent circuit modal 2. (c) Equivalent circuit modal 3. (d) Equivalent circuit modal 4.

$$i_a = \frac{\sqrt{2}U_2}{R^2 + 4\omega^2 L_t^2} \left[R \sin\left(\omega t + \frac{\pi}{6}\right) - 2\omega L_t \cos\left(\omega t + \frac{\pi}{6}\right) \right] + C e^{-(R/2L_t)t}. \tag{15}$$

The value of constant C can be obtained by taking the A-phase current value at $\omega t = (\pi/6) + \gamma$ during $(\pi/6) \sim (\pi/6) + \gamma$ period as the boundary condition.

The expressions of voltage and current during $(\pi/2) \sim (\pi/2) + \gamma$ period are easily obtained according to their voltage and current equations, and the solving method of the voltage and current expressions during $(\pi/2) + \gamma \sim (5\pi/6)$ period is similar to the solving method during $(\pi/6) \sim (\pi/6) + \gamma$ period, and the solving method of the voltage and current expressions during $(5\pi/6) \sim (5\pi/6) + \gamma$ period is similar to the solving method during $(\pi/6) + \gamma \sim (\pi/2)$ period. Using the expressions and boundary conditions of voltage and current, the generator's

output voltage and current waveforms can be obtained under the condition that no-load back EMF, synchronous inductance, rated frequency, and equivalent load resistance of the generator are known. The rated parameters of the existing prototype are shown in Table 1. In order to make the proportion of the periods more reasonable for the convenience of observation, in the simulation and experimental study, the given resistance value is 5 ohm, which is about half load. The output voltage and current waveforms of the A-phase winding within a single cycle be obtained as shown in Figure 4.

5. Numerical Simulation of Generator's Output Waveform

In the front, the AC side voltage and current waveforms of the nonsalient pole PM generator with rectified load are

TABLE 1: Rated parameters of the prototype.

Parameters	Values (kW)
Rated power	100
Synchronous inductance	0.32
End inductance	0.025
Phase back EMF	220
Rated frequency	100

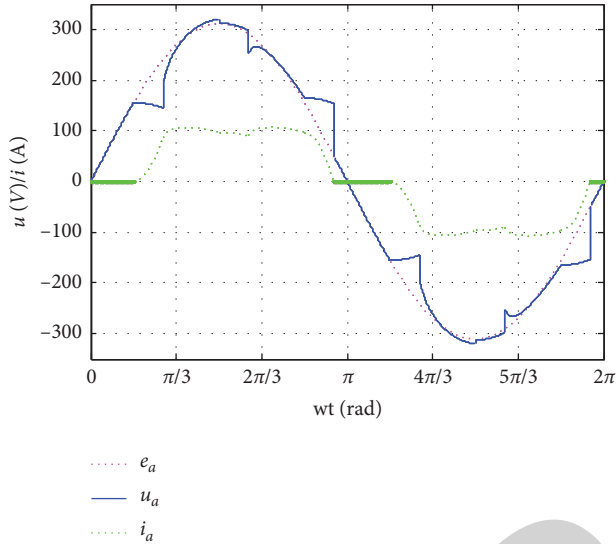


FIGURE 4: Waveforms of output voltage and current.

derived and analyzed by using the analytic method; however, this is based on a large number of idealized assumptions, and inevitably, there will be some deviations, and when the salient pole PM generator is adopted or the filter element is taken into consideration, the situation is more complicated. Because of the nonlinearity and time variation of power electronic devices, the traditional analysis methods cannot meet the requirements of static and dynamic analyses. Circuit simulation technology can be used for more accurate research, and when there is a generator in the system, the equivalent model of the generator must be established [20]. In order to facilitate the design of simulation circuit, some simulation software contains generator equivalent model. The generator's output voltage and current waveforms can be obtained by circuit simulation using the equivalent circuit of the rectifier generator set shown in Figure 1.

Although the circuit simulation method avoids the idealization assumption and approximate solution in the derivation of the generator's output voltage and current formulas, the generator is modeled equivalently, which cannot truly reflect the complex electromagnetic field of the generator changes with time and space. Without considering the influence of the harmonic magnetic field and armature reaction magnetic field on the air gap magnetic field, the influence of magnetic circuit saturation on motor parameters cannot be considered. Moreover, the accuracy of the generator parameters will directly affect the accuracy of the analysis results. The excellent performance of the finite

element method in solving such complex problems has been widely used, and the equivalent model of the generator in the circuit is replaced by the finite element model, which is changed into the field-circuit coupled simulation, and the established field-circuit coupled simulation model is shown in Figure 5. The speed of the generator is adjusted by changing the setting value of the prime mover speed-setting module. Because of the two-dimensional finite element simulation model not considering the influence of end inductance and phase resistance, the end inductance L_{aend} , L_{bend} , and L_{cend} and phase resistance R_a , R_b , and R_c shall be added to the output side of the generator. The output voltage waveforms and current waveforms of the generator obtained by means of analytic method, circuit simulation method, and field-circuit coupled simulation method are shown in Figures 6 and 7, respectively.

Figures 6 and 7 show that the current waveforms obtained by the three methods are very close, with little difference. The difference of voltage waveforms between the analytic method and circuit simulation method is very small, and the accuracy of voltage and current analytic formula and the validity of the formula deduction process are explained. The voltage waveform obtained by the field-circuit coupling simulation method is obviously different from that obtained by the other two methods, mainly in the voltage drop rate during the commutation phase and the peak value of the output voltage. The main reason is that although the air gap magnetic field of the generator has been sinusoidal, but the no-load back EMF waveform of the generator still contains harmonic components. Moreover, the armature reaction magnetic field will further lead to the asymmetry of the air gap magnetic field and weaken the air gap magnetic field in general. The influence of the impedance voltage drop will decrease the peak value of the voltage.

6. Experimental Test of Generator's Output Waveform

In order to verify the validity of the above analysis methods, the rectifier generator set experimental platform is built to measure the output waveform of the prototype. Using variable-frequency motor drives the generator operating at rated speed same as the simulation given value, and when testing, the load resistance value is adjusted to the same value as the simulation setting. The generator output voltage and current waveforms are shown in Figures 8 and 9, respectively. By comparison, it can be found that the measured voltage and current waveforms agree well with the waveforms obtained by previous methods, and waveforms obtained by the field-circuit coupled method is more close to the measured, which also explains the accuracy of the above analysis.

7. Optimization of Generator Output Waveform Quality

According to the generator's output voltage and current waveforms obtained by above methods, during the conduction phase commutation of the A phase, the existence of

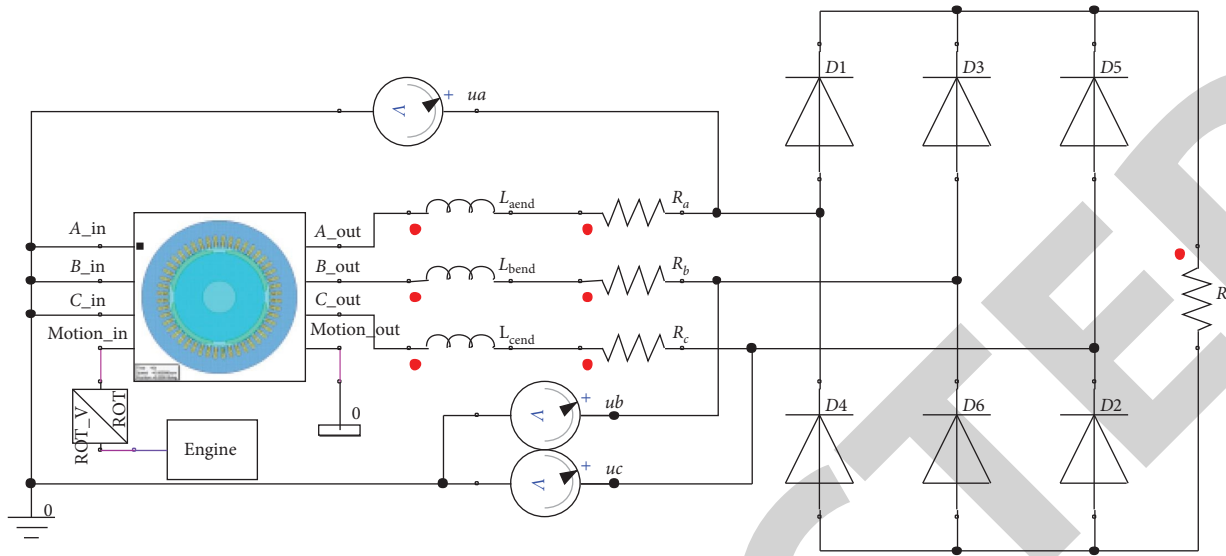


FIGURE 5: Field-circuit coupled simulation model.

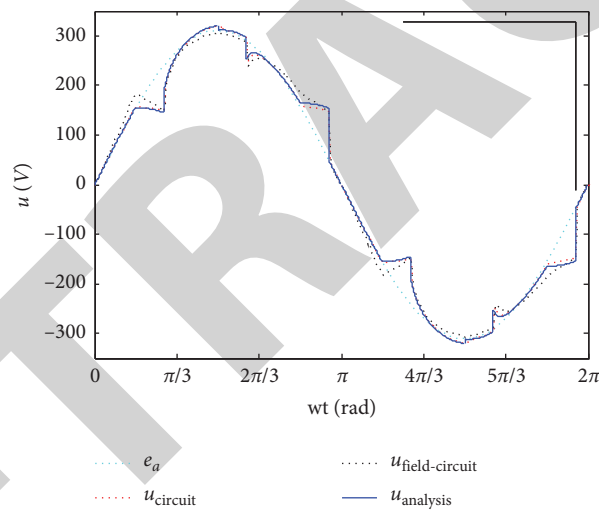


FIGURE 6: Comparison of output voltage waveforms.

the commutation overlap angle causes the voltage waveform to concave. During cut-off phase commutation of the A phase, the existence of the commutation overlap angle causes the voltage waveform to convex. During the phase commutation B and C, the voltage waveform also has a concave phenomenon. Therefore, the existence of the commutation overlap angle causes serious distortion of generator's output voltage waveform. According to the generator output current waveforms, we can see that the existence of the commutation overlap angle will lead to longer conduction time of the winding, which will result in the phase difference between the voltage waveform and the current waveform. When the synchronous inductance is different, the generator's output voltage, current waveforms, and the corresponding harmonic distortion rate are shown in Figures 10 and 11, respectively. As can be seen from Figures 10 and 11, with the increase of synchronous

inductance, the distortion of the output voltage waveform is aggravated, and the distortion of the output current waveform is improved.

In order to improve the output waveforms of the generator, the most commonly used passive filter circuit shown in Figure 12, and the inductances $L1 = L2 = L3$ series in the circuit, and the capacitors $C1 = C2 = C3$ parallel in the circuit, and the influence of the capacitance value and inductance value on the voltage and current waveforms' quality of the generator is analyzed by simulation [21].

Through the circuit simulation, the distortion rates of the voltage waveform and current waveform of the generator change with inductance and capacitance values, which are shown in Figures 13 and 14, respectively. The fundamental power factors of the generator output side change with inductance and capacitance values, which are shown in Figure 15.

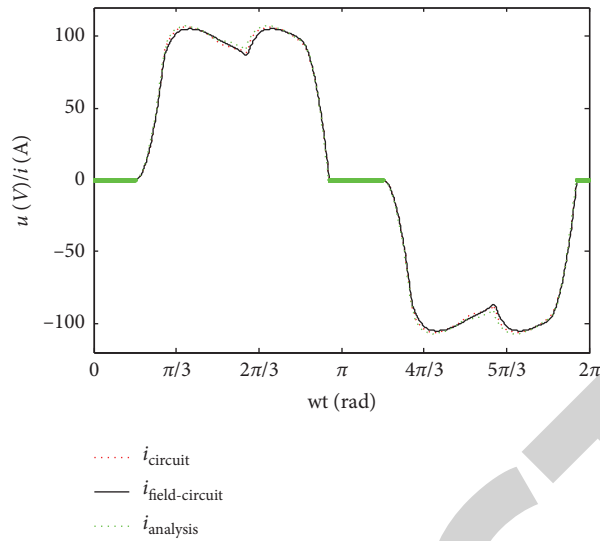


FIGURE 7: Comparison of output current waveforms.

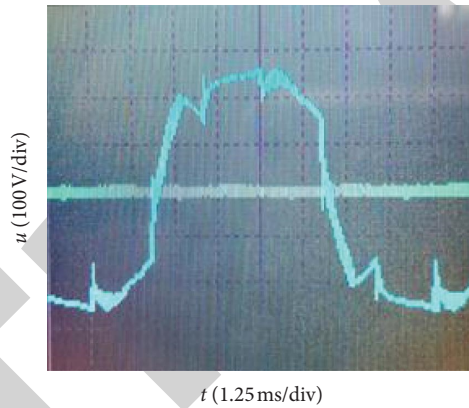


FIGURE 8: Measured output voltage waveform.

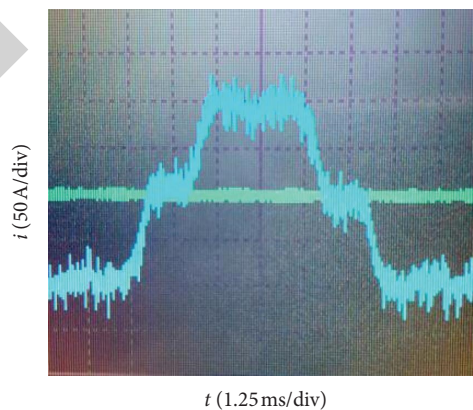


FIGURE 9: Measured output current waveform.

It can be clearly seen from Figures 13–15 that the passive filter circuit can significantly improve the quality of generator voltage and current waveforms. Increasing the filter inductance can significantly reduce the distortion rate of

voltage and current waveforms, but it will reduce the fundamental power factor. Increasing the filter capacitor can reduce the distortion rate of voltage and current waveforms and improve the fundamental power factor. High-quality

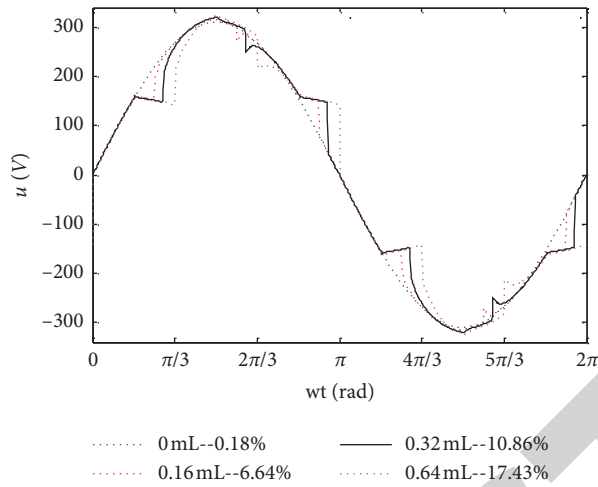


FIGURE 10: Influence of synchronous inductance on the voltage waveform.

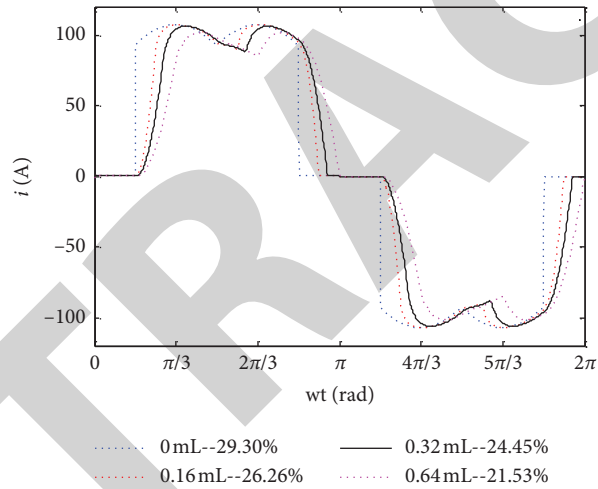


FIGURE 11: Influence of synchronous inductor on the current waveform.

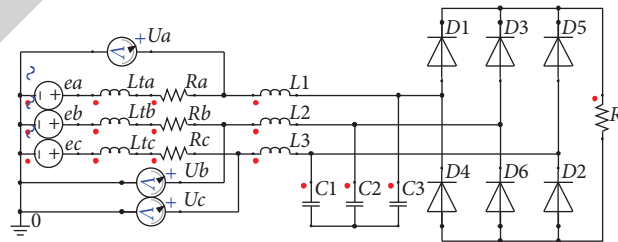


FIGURE 12: The passive filter circuit.

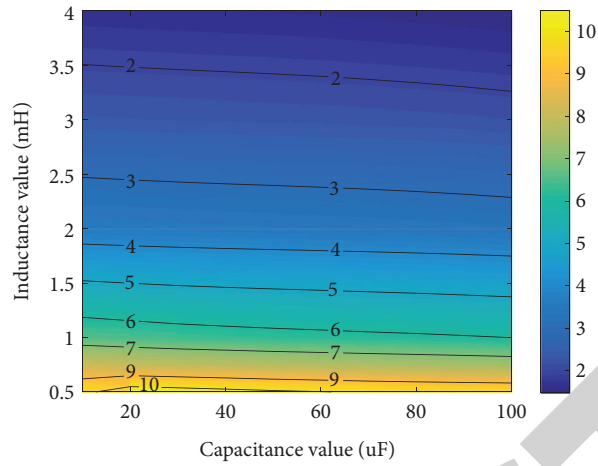


FIGURE 13: Distortion rates of the voltage waveform.

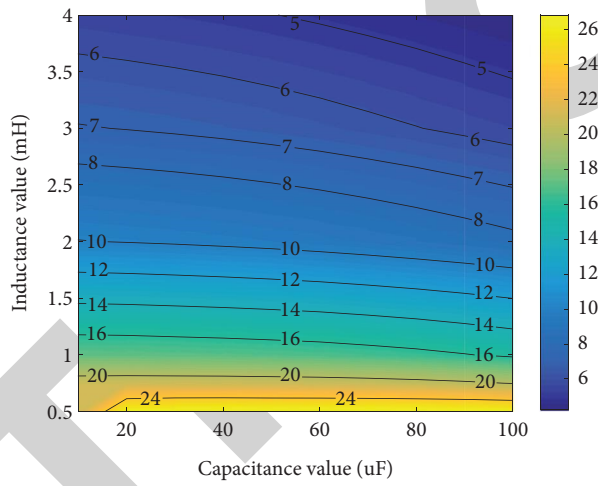


FIGURE 14: Distortion rates of the voltage waveform.

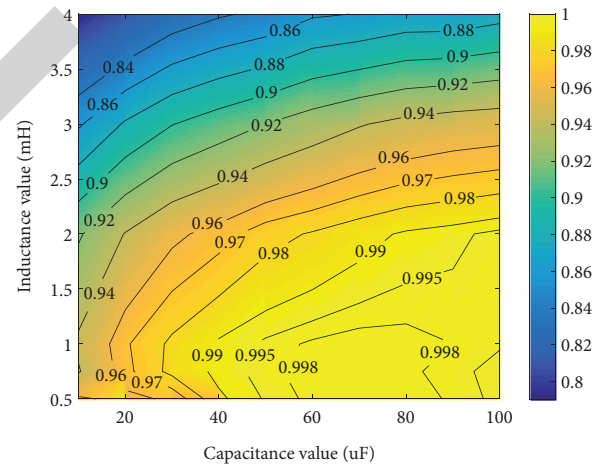


FIGURE 15: Distortion rates of the voltage waveform.

generator voltage and current waveforms and high power factor can be obtained by selecting filter capacitance and filter inductance.

8. Conclusion

The output waveform of the generator with rectifier load is studied in this paper. On the basis of the equivalent circuit, the commutation process of the uncontrolled rectifier circuit is analyzed when the commutation overlap angle is considered, and the influence of rectifier generator parameters on the commutation overlap angle is analyzed, and the analytic expression of the commutation overlap angle is given. The output voltage and current waveforms of the generator are obtained by analytic method, circuit simulation method, field-circuit coupled simulation method, and experimental method, respectively, and the advantages and limitations of these methods are explained. By comparing the output voltage and current waveforms obtained by different methods, the field-circuit coupled simulation method is in good agreement with the experimental method.

In this paper, the influence of the rectifier circuit on the output voltage and current waveforms of the generator is summarized, and the influence of synchronous inductance on the output waveform and harmonic distortion rate of the generator is analyzed. With the increase of the capacity difference between the generator and the rectifier load, the influence of the commutation overlap angle becomes smaller. The influence of the capacitance value and inductance value on the voltage and current waveforms' quality of the generator is analyzed by passive filter circuit simulation. Increasing the filter inductance can significantly reduce the distortion rate of voltage and current waveforms, but it will reduce the fundamental power factor. Increasing the filter capacitor can reduce the distortion rate of voltage and current waveforms and improve the fundamental power factor. The research of this paper has the guidance and reference significance for the application of the generator with rectifier load.

Data Availability

The data used to support the findings of this study are included within the article.

Conflicts of Interest

The authors declare that they have no conflicts of interest.

References

- [1] G. He, B. Zhang, and G. Feng, "Power balanced control of rectifier permanent magnet generator sets," *Journal of Intelligent & Fuzzy Systems*, vol. 40, no. 2, pp. 2993–3003, 2021.
- [2] P. M. Nicolae, M. Ş. Nicolae, and I. D. Nicolae, "Distorting regimes and their measurement systems for the diagnosis purposes in three-phase systems," in *Proceedings of the IEEE International Conference on the Science of Electrical Engineering (ICSEE)*, pp. 1–5, Eilat, Israel, December 2016.
- [3] S. S. Kumar, N. Kumaresan, and M. Subbiah, "Analysis and control of capacitor-excited induction generators connected to a micro-grid through power electronic converters," *IET Generation, Transmission & Distribution*, vol. 9, no. 10, pp. 911–920, 2015.
- [4] M. B. Ketzner and C. B. Jacobina, "Sensorless control technique for PWM rectifiers with voltage disturbance rejection and adaptive power factor," *IEEE Transactions on Industrial Electronics*, vol. 62, no. 2, pp. 1140–1151, 2015.
- [5] S. Sahbani, H. Mahmoudi, A. Hasnaoui, M. Kchikach, and A. Redouane, "A novel high power factor PWM rectifier with push-pull control for harmonic reduction in industrial areas networks of smart grid," in *Proceedings of the International Renewable and Sustainable Energy Conference (IRSEC)*, pp. 1080–1084, Tetouan, Morocco, November 2016.
- [6] M. Kiani and W. J. Lee, "Effects of voltage unbalance and system harmonics on the performance of doubly fed induction wind generators," *IEEE Transactions on Industry Applications*, vol. 46, no. 2, pp. 562–568, 2010.
- [7] J. Yong, A. B. Nassif, and W. Xu, "Effect of voltage crest shape on the harmonic amplification and attenuation of diode-bridge converter-based loads," *IET Generation, Transmission & Distribution*, vol. 5, no. 10, pp. 1033–1041, 2011.
- [8] S. Jordan and J. Apsley, "Diode rectification of multiphase synchronous generators for aircraft applications," in *Proceedings of the IEEE Energy Conversion Congress and Exposition*, pp. 3208–3215, Vancouver, Canada, October 2011.
- [9] Y. Zhang and Y. Wu, "Design of synchronous generator for integrated power propulsion system in marine," *Transactions of China Electrotechnical Society*, vol. 28, no. 10, pp. 67–74, 2016.
- [10] Y. Y. Sun, C. K. Dai, J. Q. Li et al., "Frequency-domain harmonic matrix model for three-phase diode-bridge rectifier," *IET Generation, Transmission & Distribution*, vol. 10, no. 7, pp. 1605–1614, 2016.
- [11] N. C. Zhou, J. J. Wang, Q. G. Wang, and N. Q. Wei, "Measurement-based harmonic modeling of an electric vehicle charging station using a three-phase uncontrolled rectifier," *IEEE Transactions on Smart Grid*, vol. 6, no. 3, pp. 1332–1340, 2015.
- [12] J. Fang, Y. Wang, L. Le, and S. N. Li, "Frequency domain harmonic model of electric vehicle charger using three-phase uncontrolled rectifier," in *Proceedings of the China International Conference on Electricity Distribution (CICED)*, pp. 1–5, Tianjin, China, September 2016.
- [13] K. Wei, D. Wang, X. W. Yu, Z. Z. Su, and S. W. Cheng, "Research on AC output characteristic of a multiphase permanent magnet generator with rectified load," in *Proceedings of the IEEE Conference and Expo Transportation Electrification Asia-Pacific (ITEC Asia-Pacific)*, pp. 1–5, Beijing, China, 2014.
- [14] J. Meyer, S. Müller, P. Schegner et al., "Comparison of methods for modelling electric vehicle chargers for harmonic studies," in *Proceedings of the Power Systems Computation Conference (PSCC)*, pp. 1–7, Genoa, Italy, June 2016.
- [15] Z. R. Zhang, J. J. Zhou, D. M. Zhu et al., "Multi-pole low speed doubly salient electro-magnetic wind turbine generator and its rectification characteristics," *Proceedings of the CSEE*, vol. 39, no. 6, pp. 67–72, 2009.
- [16] S. K. Cheng, Y. J. Yu, F. Chai et al., "Analysis of the inductances of interior permanent magnet synchronous motor," *Proceedings of the CSEE*, vol. 29, no. 18, pp. 94–99, 2009.
- [17] C. Y. Wang, J. K. Xia, and Y. B. Sun, *Modern Control Technology for Electric Machines*, pp. 104–112, China machine press, Beijing, China, 2008.

- [18] C. H. Zhang, X. Sun, W. M. Tong et al., "Calculation and measurement of transient reactance of permanent magnet synchronous motor," *Electrical Engineering*, vol. 4, pp. 14–17, 2009.
- [19] W. L. Dai, H. H. Qin, H. H. Guo et al., "Analysis of commutation in three-phase rectifier of doubly salient electromagnetic generator," *Proceedings of the CSEE*, vol. 28, no. 20, pp. 111–117, 2008.
- [20] B. J. Ge, S. Y. Xiao, Z. H. Liu et al., "Improved model of synchronous generators internal faults based on circuit-coupled FEM," *IEEE Transactions on Energy Conversion*, vol. 32, no. 3, pp. 876–884, 2017.
- [21] B. Abood Salam and M. Abdul Wahhab Thamir, "Investigation of harmonic reduction using passive filters in a distribution network in basra city," *IOP Conference Series: Materials Science and Engineering*, vol. 1, no. 1067, 2021.

RETRACTED